ALEPH/2000-068
CONF/2000-046
July 19, 2000

PRELIMINARY

Measurement of the effective b quark fragmentation function at the Z peak

ALEPH Collaboration

Corresponding author: Tommaso Boccali (Tommaso.Boccali@cern.ch)

Abstract

A model–independent study of the fragmentation of b quarks into B mesons is presented. The analysis makes use of the statistics collected by the ALEPH experiment at and around the Z peak during the years 1991–1995, which corresponds to almost four million hadronic Z decays. A semi–exclusive reconstruction of $B \to l\nu D^{(\star)}$ decays is performed, by combining lepton candidates with fully reconstructed $D^{(\star)}$ mesons, while the neutrino energy is estimated from the missing energy of the event.

The mean value of x_b^{L}, the reduced energy of the leading B meson after fragmentation, is found to be

$$\langle x_b^{\mathrm{L}} \rangle = 0.7499 \ \pm 0.0065\,(\mathrm{stat}) \ \pm 0.0069\,(\mathrm{syst})$$

The distribution for x_b^{L} is also compared with a number of different fragmentation models.

ALEPH Contribution for ICHEP 2000

1 Introduction

In high energy processes which involve strong interactions the quarks are not observed as free particles, but appear as jets of colourless hadrons. The energy of the first (*leading*) B hadron after the *fragmentation* process is the subject of this study. The process of hadron production is described as the convolution of a perturbative part (gluon radiation with $Q^2 > 1$ GeV) and the non–perturbative fragmentation process itself, which is usually parametrised in terms of the variable z:

$$z \equiv \frac{\left(E + p_{||}\right)_{\text{hadron}}}{(E+p)_{\text{quark}}} \quad , \tag{1}$$

where $p_{||}$ is the hadron's momentum along the direction of the quark, and $(E+p)_{\text{quark}}$ is the sum of energy and momentum of the quark just before fragmentation, i.e. taking into account initial and final state radiation, and hard gluon emission.

The results should be expressed in terms of the probability of a B hadron to be generated with a given z, called $D_Q^H(z)$.

Unfortunately z is not accessible experimentally on an event by event basis, and hence a direct reconstruction of $D_Q^H(z)$ is not possible. The energy spectrum of B hadrons can also be described in terms of the *scaled mean energy* x_b^{L}, defined as the ratio of the *leading* heavy hadron energy to the beam energy

$$x_b^{\text{L}} \equiv \frac{E_{\text{lead. had.}}}{E_{\text{beam}}} \quad . \tag{2}$$

The main difference to the z variable is in the denominator, because E_{beam} does not unfold the effects of initial and final state radiation and hard gluon emission.

In the analysis presented, the energy distribution of B mesons is reconstructed using a semi–exclusive method: semileptonic decays of $B \to l\nu_l D^{(\star)}$ are identified by pairing lepton candidates with fully reconstructed $D^{(\star)}$ mesons; the reduced energy of the *weakly* decaying B meson, x_b^{reco}, is then computed adding an estimate of the neutrino energy.

Five channels are chosen because of their good signal purity and statistical significance; they are shown in Table 1.

In the following x_b^{reco} and x_b^{wd} indicate the reconstructed and true reduced energy of the weakly–decaying B meson, respectively; x_b^{L} stands for the reduced energy of the leading B meson.

Table 1: B–decay channels used in the analysis.

Number	Channel
1	$B^0 \to l\nu D^\star; \quad D^\star \to D^0\pi_s; \quad D^0 \to K\pi$
2	$B^0 \to l\nu D^\star; \quad D^\star \to D^0\pi_s; \quad D^0 \to K\pi\pi\pi$
3	$B^- \to l\nu D^0; \quad D^0 \to K\pi$
4	$B^0 \to l\nu D; \quad D \to K\pi\pi$
5	$B^0 \to l\nu D^\star; \quad D^\star \to D^0\pi_s; \quad D^0 \to K\pi\pi^0$

After a brief description of the ALEPH detector, the selection of $B \to l\nu D^{(\star)}$ is explained in Section 3. In Section 4 the reconstruction of the B meson energy is presented, followed by

the extraction of the spectrum and the comparison with the predictions of different models in Section 5. Systematic uncertainties are discussed in Section 6, and checks on the robustness of the analysis are presented in Section 7.

2 The ALEPH detector

The ALEPH detector is described in detail elsewhere [1]. A high resolution vertex detector (VDET) consisting of two layers of silicon with double–sided readout provides measurements in the $r\phi$ and z directions at average radii of 6.5 cm and 11.3 cm, with 12 μm precision at normal incidence. The VDET provides full azimuthal coverage, and polar angle coverage to $|\cos\theta| < 0.85$ for the inner layer and $|\cos\theta| < 0.69$ for both layers. Outside VDET, particles traverse the inner tracking chamber (ITC) and the time projection chamber (TPC). The ITC is a cylindrical drift chamber with eight axial wire layers at radii of 16 to 26 cm. The TPC measures up to 21 space points per track at radii between 40 and 171 cm, and also provides a measurement of the specific ionization energy loss (dE/dx) of each charged track. These three detectors form the tracking system, which is immersed in a 1.5 T axial magnetic field provided by a super-conducting solenoid. The combined tracking system yields a momentum resolution of $\sigma(1/p_T) = 6 \times 10^{-4}$ (GeV/c)$^{-1}$. The resolution of the three–dimensional impact parameter in the $r\phi$ and z views for tracks having two VDET hits can be parameterised as $\sigma = 25$ μm$+95\mu$m$/p$, (p in GeV/c).

The electromagnetic calorimeter (ECAL) is a lead/wire chamber sandwich operated in proportional mode. The calorimeter is read out in projective towers that subtend typically $0.9^\circ \times 0.9^\circ$ in solid angle, segmented in three longitudinal sections. The hadron calorimeter (HCAL) uses the iron return yoke as absorber. Hadronic showers are sampled by 23 planes of streamer tubes, with analog projective tower and digital hit pattern readout. The HCAL is used in combination with two layers of muon chambers outside the magnet for muon identification.

Recently the LEP I data set has been reprocessed using improved reconstruction algorithms. The main benefits for this analysis are related to the enhanced secondary vertex reconstruction efficiency and the improved particle identification. In particular a new VDET pattern recognition algorithm allows for groups of several nearby tracks which may share common hits being analysed together, in order to find the hit–to–track assignment which minimise the χ^2 for the event as a whole. The improvement on the hit association efficiency is more than 2%.

Information from the TPC wires, in addition to the one obtained from the pads, is used to improve the coordinate resolution by a factor of two in z, while a 30% improvement for low momentum tracks is achieved in $r\phi$.

In order to enhance the particle identification capability, the pulse height data of the TPC pads, unambiguously available for almost all tracks, is now used to complement and improve the information from the sense wires, available only for about 85% of the tracks.

3 Selection of $B \to l\nu D^{(\star)}$ decays

The analysis uses the full LEP I statistics collected by ALEPH between 1991 and 1995, which amounts to almost four million hadronic Z decays.

A Monte Carlo simulation based on JETSET 7.4 [2] has been used in order to get information about resolution functions, acceptance corrections and background compositions: this amounts to about five million $b\bar{b}$ events and more than twice the data statistics of $q\bar{q}$ events.

The present analysis uses $b\bar{b}$ events to determine the $x_b^{\rm wd}$ and $x_b^{\rm L}$ spectrum starting from reconstructed $x_b^{\rm reco}$ spectra, and $q\bar{q}$ events to evaluate the *non-*$b\bar{b}$ component of the selected sample.

The decays $B \to l\nu D^{(\star)}$ are searched for in hadronic events, containing at least one lepton (electron or muon) identified using standard criteria [3]. The transverse momentum p_T of the lepton with respect to the jet to which it belongs, is required to be larger than 1 GeV/c, which helps rejecting fake leptons and leptons not coming from direct decays of b hadrons.

Events are divided in two hemispheres using the thrust axis; in each hemisphere a D meson is reconstructed in the decay modes described in Table 1, by combining tracks which belong to the lepton hemisphere. At least two charged tracks from the D meson decay are required to be associated to VDET hits, in order to ensure a good reconstruction of the D vertex position and reject combinatorial background. Loose cuts are applied to track momenta, in order to limit the bias in the B momentum distribution. Tracks are not considered as kaon candidates if their measured ionization is incompatible with the kaon hypothesis by more than three standard deviations. The charge of the kaon candidate is required to be the same as the one of lepton, as expected for semileptonic B meson decays.

Tracks from the D meson decay are fitted to a common vertex, and the track combination is rejected if the χ^2 of the fit is larger than 20. For channels 3 and 4, if more than one combination fulfils this requirement, the one with the smallest χ^2 is chosen. In channel 5, the π^0 closest in angle to the charged pion is selected and added to form the D^0.

For channels 1, 2 and 5, a *soft* pion $\pi_{\rm s}$ is added to the D candidate to form a $D^\star$ meson; the $\pi_{\rm s}$ momentum is required to be larger than 250 MeV and smaller than 3 GeV.

In each hemisphere, the track combination with the smallest mass difference $M(D\pi) - M(D^\star)$ is taken as the $D^\star$ candidate.

A fit is performed using the D candidate and the lepton tracks, and again the combination of tracks is rejected if the χ^2 of the fit is larger than 20. The B vertex is required to lie between the interaction point, reconstructed event by event, and the D vertex.

The channels 3 and 4, without a $D^\star$, are additionally enriched in $b\bar{b}$ events using harder dE/dx cuts on the kaon; in addition a $\pi_{\rm s}$ veto is applied: if a track is found which is compatible with the reconstructed B vertex and whose 4–momentum is consistent with the kinematics of a $D^\star$ decay, the track combination is discarded. Finally, harder cuts on the D mass and the vertex fit χ^2 are imposed.

The purity of the selected events is calculated from the data, by fitting the reconstructed $D^{0/\pm}$ mass peak in a window between 1.7 and 2.0 GeV, assuming a linear function for the background and a gaussian shape for the signal.

The $D^{0/\pm}$ mass spectra are shown in Fig. 1. The number of events in the selection window, with the purity from the fit, are given in Table 2.

Purities and widths are well reproduced in the Monte Carlo simulation, at a level of 5%; this is taken into account in the evaluation of systematic uncertainties.

Table 2: Number of selected events, purities and D mass resolution for the five channels.

Channel	D window (GeV)	Events	Resolution (MeV)	Purity(%)
$D^0 \to K\pi(D^\star)$	1.864 ± 0.030	665	8.7	89
$D^0 \to K\pi\pi\pi(D^\star)$	1.864 ± 0.030	381	6.4	69
$D^0 \to K\pi$	1.864 ± 0.015	706	8.4	81
$D^- \to K\pi\pi$	1.869 ± 0.030	303	7.6	68
$D^0 \to K\pi\pi^0(D^\star)$	1.864 ± 0.050	693	26	63

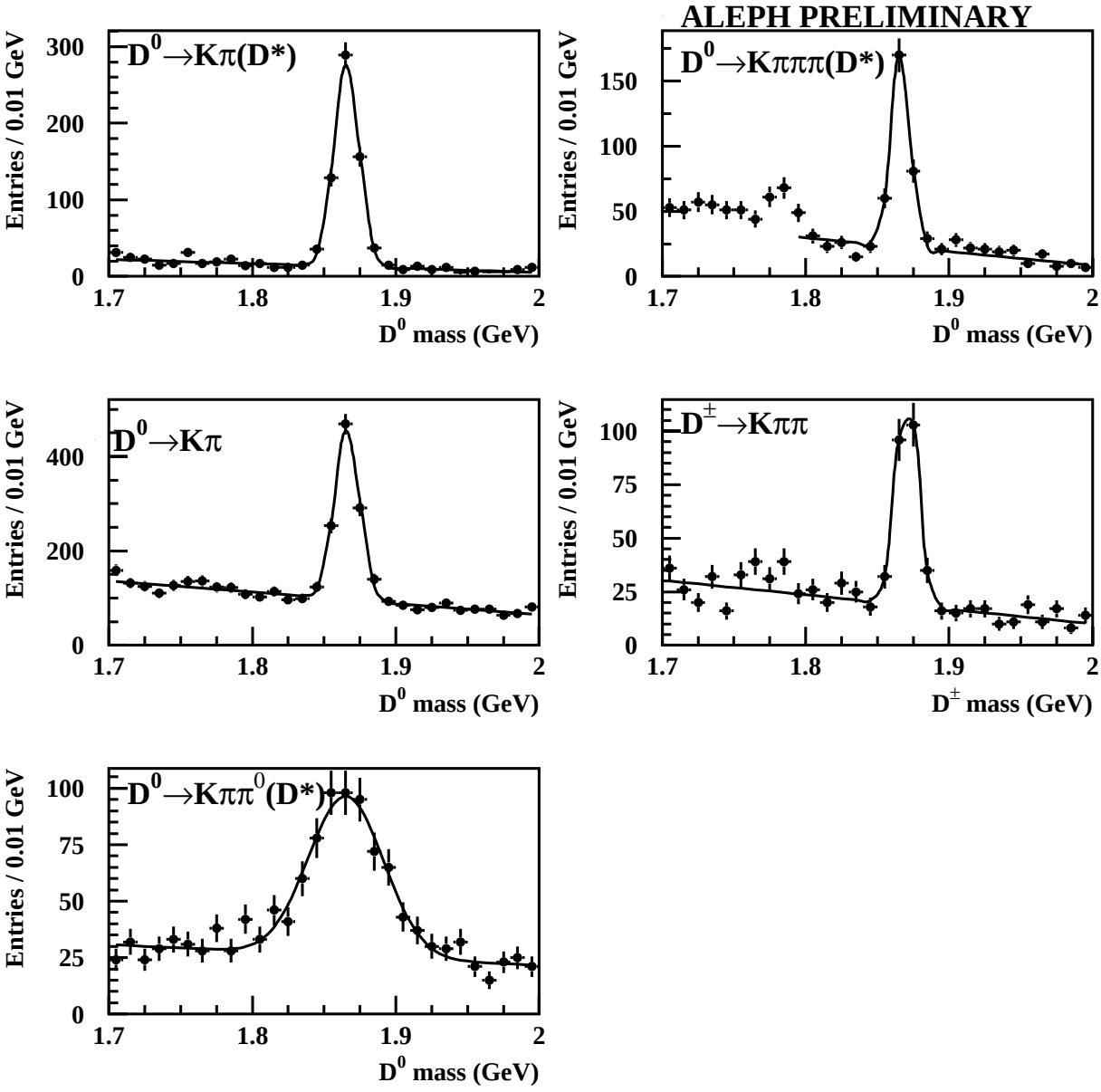

Figure 1: Reconstructed $D^{0/\pm}$ mass peaks in the five channels.

4 B energy reconstruction

The energy of the weakly decaying $B \to l\nu_l D^{(\star)}$ hadron is estimated as

$$x_b^{\rm reco} = \frac{E_l + E_{D^{(\star)}} + E_\nu}{E_{\rm beam}} \ . \tag{3}$$

The terms $E_{D^{(\star)}}$ and E_l are easily estimated using direct reconstruction methods; this cannot be done for the neutrino energy E_ν, which must be evaluated using a missing energy technique in the hemisphere of the lepton:

$$E_\nu = E_{\rm tot}^{\rm hemi} - E_{\rm vis}^{\rm hemi} \tag{4}$$

A good resolution on E_ν can be obtained by using information also from the hemisphere opposite to the lepton and from energy–momentum conservation. This leads to

$$E_{\rm tot}^{\rm hemi} = E_{\rm beam} + \frac{m_{\rm same}^2 - m_{\rm oppo}^2}{4E_{\rm beam}} \tag{5}$$

where the invariant masses $m_{\rm same}$ and $m_{\rm oppo}$ are computed using all the particles in the same and opposite hemispheres with respect to the lepton hemisphere. The resolution depends on $x_b^{\rm reco}$. For events selected in channel 1, it varies from 2.6 GeV for $x_b^{\rm reco} < 0.5$ to 0.9 GeV for $x_b^{\rm reco} > 0.9$.

Table 3 shows Monte Carlo resolutions for $\left(x_b^{\rm wd} - x_b^{\rm reco}\right)$ obtained from selected events for $b\bar{b}$ events only; the resolution shapes are fitted with two gaussians, accounting for core and tails.

Table 3: Monte Carlo resolution for $(x_b^{\rm wd} - x_b^{\rm reco})$; the resolution can be parameterised with two gaussians, the first one describing the core and the second the tails.

Channel	Core (%)	Core resolution	Tails (%)	Tails resolution
$D^0 \to K\pi(D^\star)$	52	0.03	48	0.10
$D^0 \to K\pi\pi\pi(D^\star)$	51	0.04	49	0.12
$D^0 \to K\pi$	59	0.04	41	0.15
$D^- \to K\pi\pi$	57	0.04	43	0.14
$D^0 \to K\pi\pi^0(D^\star)$	55	0.04	45	0.12

5 Unfolding methods

The raw reduced energy distribution for the weakly decaying B meson ($x_b^{\rm reco}$) is reconstructed in 20 bins between 0 and 1. In each of them, the *non-$b\bar{b}$* background is estimated using Monte Carlo events, and subtracted from the spectrum. This amounts to about 2% of the events. The corrected spectra are shown in Fig. 2.

With these events two different kinds of analyses can be performed:

- a *model–dependent* analysis, in which fragmentation models present in literature are compared to the data;
- a *model–independent* analysis, in which the shape of $x_b^{\rm L}$ is reconstructed correcting the spectra for acceptance, detector resolution and missing particles.

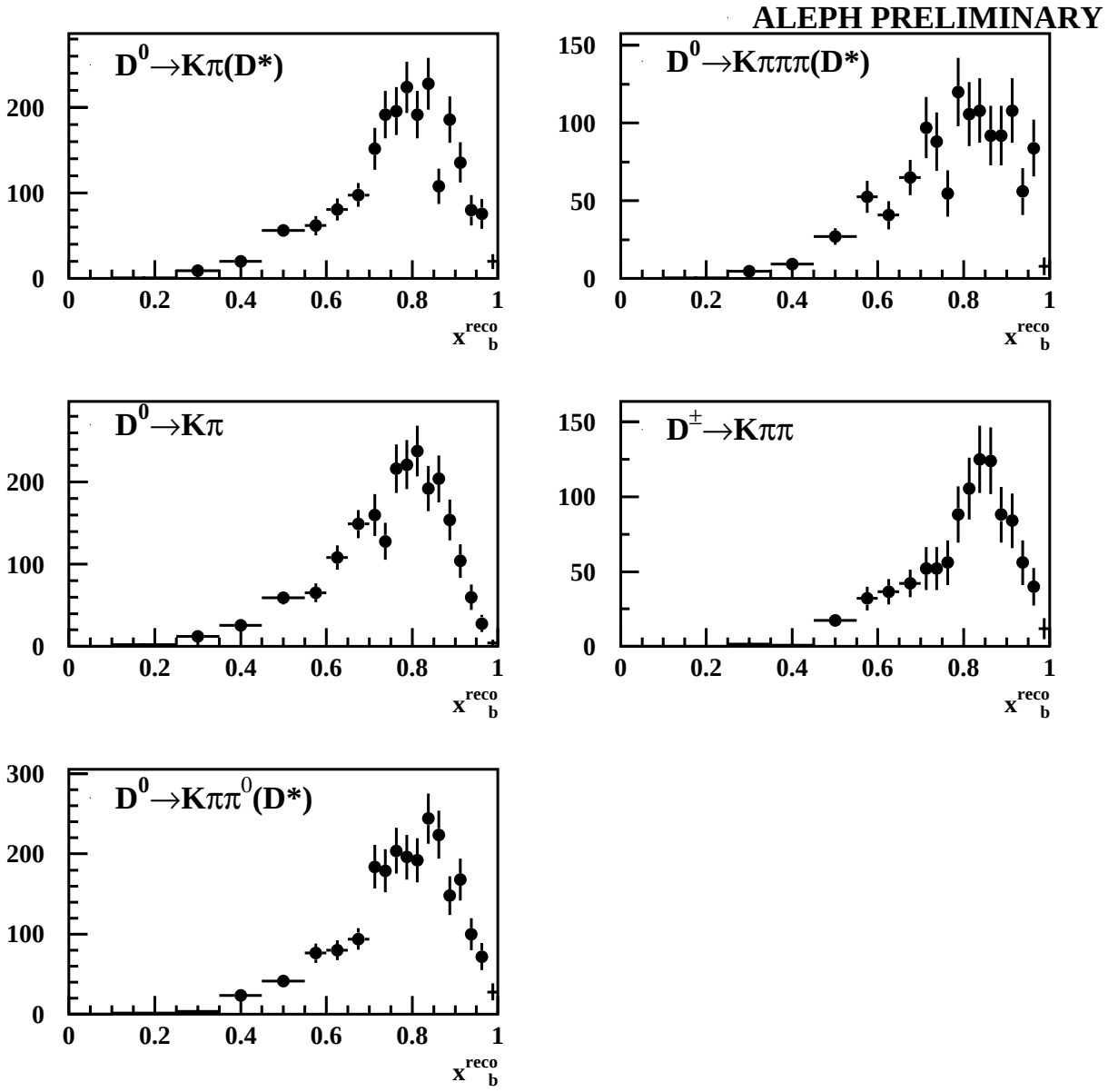

Figure 2: Reconstructed $x_b^{\rm reco}$ spectra in the five channels, before acceptance corrections, but after $non - b\bar{b}$ background subtraction.

5.1 Model–dependent analysis

In this analysis the shape of $D_b^H(z)$ is imposed in the Monte Carlo generator JETSET 7.4 [2], which accounts for the simulation of initial and final state radiations. The reconstructed spectra obtained from the simulation ($b\bar{b}$ events only) are compared with the $x_b^{\rm reco}$ spectra from data events, using a χ^2 technique. The following parameterisations for $D_b^H(z)$ were tried:

$$\begin{aligned}
\text{Peterson et al.[5]}: \quad & D_b^H(z) \propto \frac{1}{z}\left(1-\frac{1}{z}-\frac{\epsilon_B}{1-z}\right)^{-2} \\
\text{Kartvelishvili et al.[6]}: \quad & D_b^H(z) \propto z^{\alpha_b}\,(1-z) \\
\text{Collins et al.[7]}: \quad & D_b^H(z) \propto \left(\frac{1-z}{z}+\frac{(2-z)\,\epsilon_B}{1-z}\right)\left(1+z^2\right)\left(1-\frac{1}{z}-\frac{\epsilon_B}{1-z}\right)^{-2}
\end{aligned}$$

The minimisation is performed with respect to the only parameter of the model, using every bin i for each channel c:

$$\chi^2 = \sum_{c=1}^{5}\sum_{i=1}^{20} \frac{\left((x_b^{\rm reco})^{DT}(c,i) - (x_b^{\rm reco})^{MC}(c,i)\right)^2}{\sigma_{DT}^2(c,i)+\sigma_{MC}^2(c,i)} \quad . \tag{6}$$

Table 4 reports the central values for the different parameters, together with statistical and the systematic uncertainties from physics knowledge (branching ratios and decay models) that will be discussed in Section 6.

Table 4: Model–dependent analysis. The systematic uncertainty includes the physics sources treated in Section 6.

Model	Best fit	$\langle x_b^{\rm L}\rangle$	χ^2/N_{DOF}
Peterson[5]	$\epsilon_B = 0.0022 \pm 0.0003 \pm 0.0004$	$0.733 \pm 0.004 \pm 0.005$	116/94
Kartvelishvili[6]	$\alpha_\beta = 16.0 \pm 1.2 \pm 2.1$	$0.746 \pm 0.004 \pm 0.007$	97/94
Collins[7]	$\epsilon_B = 0.00105 \pm 0.00024 \pm 0.00027$	$0.712 \pm 0.005 \pm 0.005$	164/94

The fragmentation function by Kartvelishvili gives a good agreement with data, while the function by Peterson still gives an acceptable fit. The fragmentation function by Collins is not able to reproduce the data.

5.2 Model–independent analysis

In this analysis the shape of the $x_b^{\rm L}$ spectrum is obtained by correcting the reconstructed $x_b^{\rm reco}$ spectra for acceptance, detector resolution and missing particles.

The normalised binned spectrum $f_i\left(x_b^{\rm L}\right)$ can be obtained using the relation

$$f_i\left(x_b^{\rm L}\right) = \frac{\sum_{c=1}^{5}\frac{1}{\epsilon_i(c)}\sum_{j=1}^{20} G_{ij}(c)\left(x_b^{\rm reco}(c)\right)_j}{T} \tag{7}$$

in which $\epsilon_i(c)$ is the acceptance of bin i for channel c, $\left(x_b^{\rm reco}(c)\right)_j$ is the number of reconstructed B mesons in data for channel c, with an energy in the range of bin j, and $G_{ij}(c)$ is the resolution

matrix that links mesons with $x_b^{\rm reco}$ in bin j and $x_b^{\rm L}$ in bin i, for channel c; it is taken from Monte Carlo simulation. T is the normalisation factor in order to assure $\sum_i f_i = 1$.

Equation 7 cannot guarantee a complete independence from the Monte Carlo used, since some dependence remains because of G_{ij}; hence, the Monte Carlo used to calculate G_{ij} must be reweighted to the *best guess* of $f_i\left(x_b^{\rm L}\right)$ in data. This is done using an iterative procedure, calculating $f_i^N\left(x_b^{\rm L}\right)$ for each iteration N using the G_{ij}^{N-1} from Monte Carlo reweighted to $f_i^{N-1}\left(x_b^{\rm L}\right)$. To avoid fluctuations due to the limited statistics in data events, the weights used to generate G_{ij}^N are smoothed with a polynomial function of fifth order. The whole procedure is then repeated till convergence.

The iterative procedure was missing from the result presented by ALEPH in reference [8]; hence, the values here presented supersede those results.

Due to the iterative procedure, it is not possible to use eqn. 7 to calculate statistical errors and correlation matrices; instead, 20×5 analyses are repeated, varying each time one of the quantities $\left(x_b^{\rm reco}(c)\right)_j$ by one statistical sigma. The results obtained for $f_i\left(x_b^{\rm wd}\right)$ are then combined to give the full statistical error matrix E_{ij}:

$$E_{ij} = \sum_{c=1,5;k=1,20} (f_i^{(ck)} - f_i^{STD})(f_j^{(ck)} - f_j^{STD}) \tag{8}$$

where $f_i^{(ck)}$ is the result of the convergence for f_i when $\left(x_b^{\rm reco}(c)\right)_k$ is changed by one statistical sigma. The results, together with the statistical and systematic uncertainties, are given in Table 6.

Using the $x_b^{\rm L}$ spectrum it is possible to calculate the mean value $\langle x_b^{\rm L} \rangle$

$$\langle x_b^{\rm L} \rangle = \sum_{i=1}^{20} x_i f_i\left(x_b^{\rm L}\right) \tag{9}$$

where x_i is the mean value of $x_b^{\rm L}$ in bin i. The use of this binned relation introduces a negligible *bias* in the value of $\langle x_b^{\rm L} \rangle$. The statistical error on $\langle x_b^{\rm L} \rangle$ is given using the same procedure used for the f_i distribution.

The result for $\langle x_b^{\rm L} \rangle$ is

$$\langle x_b^{\rm L} \rangle = 0.7499 \pm 0.0065\,(stat)\,.$$

6 Systematic uncertainties

Systematic uncertainties because of detector simulation, physics and the analysis method have been studied.

Systematic uncertainties due to physics knowledge were evaluated with a Monte Carlo reweighting technique, by allowing each quantity to vary within its experimental error, and then taking the total difference as the systematic uncertainty. The reweighting affects both the resolution matrix $G_{ij}(c)$ and the acceptance corrections $\epsilon_i(c)$, that are varied simultaneously. The sources taken into account are

- Missing particles from $B^{\star\star}$ production: the fraction $b \to B^{\star\star}$ has been varied within its experimental error: $f_{B^{\star\star}} = 0.279 \pm 0.059$ [9, 10]; the systematic uncertainty is $\Delta\langle x_b^{\rm L}\rangle = 0.0025$.

- Modelling of $B^{\star\star}$ production: from spin counting, the relative abundances of $(B_1, B_0^\star, B_1^\star, B_2^\star)$ should be (3,1,3,5) [11]; changing it to (1,1,1,1) gives a systematic error of $\Delta\langle x_b^{\rm L}\rangle = 0.0005$. This systematic uncertainty, as well as the one before, is not affecting the measurement of $\langle x_b^{\rm wd}\rangle$.

- Semileptonic decays of B mesons: the current experimental knowledge [12, 13] of the semileptonic branching ratios of B mesons is summarised in Table 5. The sum of the exclusive (or semi–exclusive) rates is consistent within errors with the inclusive measurement of $BR(B \to \ell\nu X)$. The analysis is not sensitive to the total $BR(B \to \ell\nu X)$ rate, but is affected by a change in the relative rates of the different components, since these contribute in different way to the average acceptance corrections and resolution matrix.

  Six systematic uncertainties were calculated using the values in table 5:

  1. The inclusive rate of $BR(B \to \ell\nu D^{(\star)}X)$ was varied by its experimental error: $\Delta\langle x_b^{\rm L}\rangle = 0.0021$.
  2. The rate for the *narrow* D_1 state was changed by its experimental error, fixing the total $BR(B \to \ell\nu D^{(\star)})X$ to the nominal value: $\Delta\langle x_b^{\rm L}\rangle = 0.0001$.
  3. The rate for the *narrow* $D_2^\star$ state was changed by its experimental error, fixing the total $BR(B \to \ell\nu D^{(\star)}X)$ to the nominal value: $\Delta\langle x_b^{\rm L}\rangle = 0.0001$.
  4. The *wide* $D^{\star\star}$ states, not measured yet, were put to zero, compensating with the *non–resonant* $\ell\nu D^{(\star)}\pi$ states and thus fixing the total $BR(B \to \ell\nu D^{(\star)}X)$ to the nominal value: $\Delta\langle x_b^{\rm L}\rangle = 0.0011$.
  5. The $BR(B \to \ell\nu D)$ rate was changed by its experimental error: $\Delta\langle x_b^{\rm L}\rangle = 0.0003$.
  6. The $BR(B \to \ell\nu D^\star)$ rate was changed by its experimental error: $\Delta\langle x_b^{\rm L}\rangle = 0.0009$.

Table 5: Exclusive branching ratios for the $B \to \ell\nu X$ process [12, 13]: the sum is consistent with the measurement of the inclusive $B \to \ell\nu X$ rate.

Process	BR(%)
$B \to D\ell\nu$	1.95 ± 0.27
$B \to D^\star\ell\nu$	5.05 ± 0.25
$B \to D^{(\star)}X\ell\nu$	2.7 ± 0.7
with $B \to D_1\ell\nu$	0.63 ± 0.11
with $B \to D_2^\star\ell\nu$	0.23 ± 0.09
$b \to u\ell\nu$	0.15 ± 0.10
$\sum B \to \ell\nu X$	9.85 ± 0.80
Inclusive $B \to \ell\nu X$	10.18 ± 0.39

Systematic uncertainties due to detector simulation and reconstruction were taken into account:

- Neutrino energy reconstruction: a possible *bias* in eqn. 4 was checked by computing the neutrino energy for hemispheres containing a high p_T lepton, and thus a neutrino. Both the shape and the central value are well in agreement between data and Monte Carlo. The shift of 20 MeV in the mean values should be added to the $x_b^{\rm L}$ spectrum, and so the systematic is $\Delta\langle x_b^{\rm L}\rangle = 0.0004$.

- Vertexing and reconstruction: if the purity and the kinematic properties of the selected candidates are not well described by the simulation, the acceptance corrections and resolution matrices can be inadequate. In order to check for these effects, the distributions of the χ^2 probability for the reconstructed D vertices is compared, channel by channel, with the simulation. Small differences are observed, and the Monte Carlo distribution is reweighted to reproduce the data, taking the shift in the reconstructed average energy as systematic uncertainty. The resulting error estimate is $\Delta\langle x_b^{\rm L}\rangle = 0.0001$. Furthermore, the reconstructed D mass distributions in data and Monte Carlo are compared. In simulated events the widths of the mass peaks are found to be $5-10\%$ smaller, while the purity of the gaussian components, estimated from the fit to the sidebands, agree within their statistical error of about 5%. The mass cuts reported in Table 2 are varied to account for both effects, taking the total shift in the extracted energy spectrum as systematic uncertainty. The resulting estimates are respectively $\Delta\langle x_b^{\rm L}\rangle = 0.0009$ and $\Delta\langle x_b^{\rm L}\rangle = 0.0031$.

Systematic uncertainties due to the analysis method:

- Background subtraction: as previously explained, a bin–by–bin subtraction of events not coming from $b\bar{b}$ events is performed before deriving the $x_b^{\rm L}$ spectrum. The analysis is repeated without this subtraction, and half of the difference is taken as systematic uncertainty, giving $\Delta\langle x_E^b\rangle = 0.0038$.

- Monte Carlo statistics: the Monte Carlo statistics is larger than in data by a factor of 5; to evaluate a systematic effect, acceptance corrections $\epsilon_i(c)$ and $G_{ij}(c)$ elements were permitted to vary randomly by their statistical error in a series of toy experiments. The scatter of the results for $\langle x_b^{\rm L}\rangle$ is taken as systematic uncertainty because of Monte Carlo statistics: $\Delta\langle x_E^b\rangle = 0.0030$.

Adding in quadrature all systematic contributions, the measurement of $x_b^{\rm L}$ is

$$\langle x_E^b\rangle = 0.7499 \pm 0.0065\,(stat) \pm 0.0069\,(syst) \quad .$$

A similar analysis has been performed reconstructing not the reduced energy $x_b^{\rm L}$ of the *leading* B hadron, but the $x_b^{\rm wd}$ of the *weakly decaying* B hadron. The method is the same, and all the systematics taken into account for $x_b^{\rm L}$ were considered, apart from those due to $B^{\star\star}$ states which are not relevant in this case. The mean value for the energy of the weakly decaying B meson is found to be

$$\langle x_b^{\rm wd}\rangle = 0.7304 \pm 0.0062({\rm stat}) \pm 0.0058({\rm syst}) \quad .$$

and the $f_i\left(x_b^{\rm wd}\right)$ spectrum is shown in Table 7 and in Fig. 4.

Table 6: The $f_i\left(x_b^{\rm L}\right)$ binned distribution. Note that the first bin has $f_0\left(x_b^{\rm L}\right) = 0$ by definition, because a B hadron cannot have an energy lower than 5 GeV.

Bin	Range	$f_i\left(x_b^{\rm L}\right)$
1	$0 - 0.1$	0.
2	$0.10 - 0.25$	$0.008 \pm 0.000 \pm 0.005$
3	$0.25 - 0.35$	$0.019 \pm 0.007 \pm 0.003$
4	$0.35 - 0.45$	$0.037 \pm 0.005 \pm 0.004$
5	$0.45 - 0.55$	$0.065 \pm 0.005 \pm 0.006$
6	$0.55 - 0.60$	$0.048 \pm 0.006 \pm 0.003$
7	$0.60 - 0.65$	$0.057 \pm 0.004 \pm 0.003$
8	$0.65 - 0.70$	$0.072 \pm 0.004 \pm 0.004$
9	$0.70 - 0.725$	$0.045 \pm 0.004 \pm 0.003$
10	$0.725 - 0.75$	$0.050 \pm 0.002 \pm 0.003$
11	$0.75 - 0.775$	$0.054 \pm 0.002 \pm 0.003$
12	$0.775 - 0.80$	$0.063 \pm 0.002 \pm 0.003$
13	$0.80 - 0.825$	$0.070 \pm 0.003 \pm 0.003$
14	$0.825 - 0.85$	$0.077 \pm 0.003 \pm 0.003$
15	$0.85 - 0.875$	$0.082 \pm 0.003 \pm 0.003$
16	$0.875 - 0.90$	$0.083 \pm 0.003 \pm 0.004$
17	$0.90 - 0.925$	$0.079 \pm 0.003 \pm 0.006$
18	$0.925 - 0.95$	$0.060 \pm 0.004 \pm 0.006$
19	$0.95 - 0.975$	$0.029 \pm 0.003 \pm 0.004$
20	$0.975 - 1.00$	$0.003 \pm 0.001 \pm 0.001$

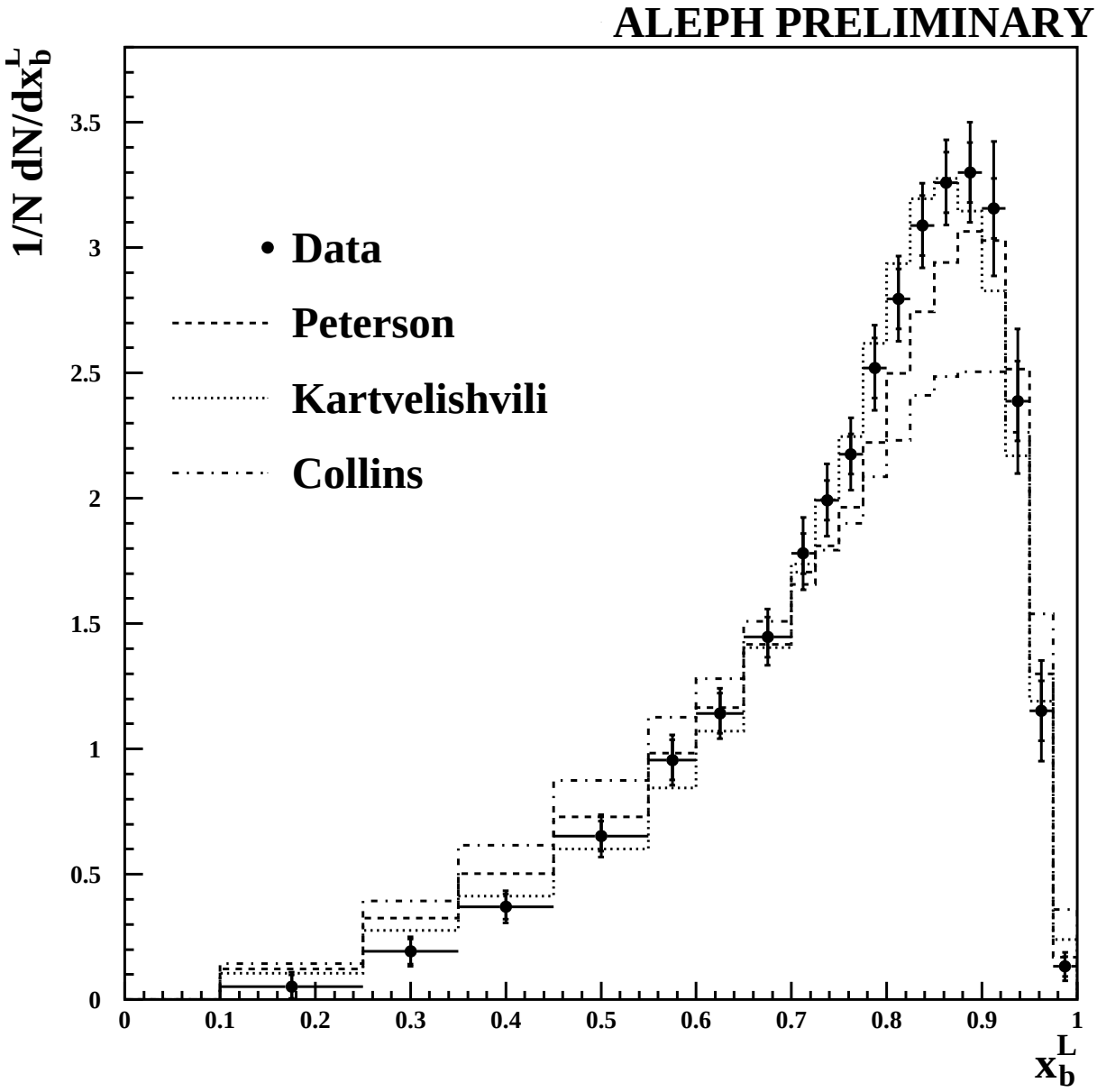

Figure 3: Reduced energy of the leading B hadron, as reconstructed from data. The smaller error bars are statistical, the wider total errors. The best–fit distributions for Peterson[5], Kartvelishvili[6] and Collins[7] are superimposed.

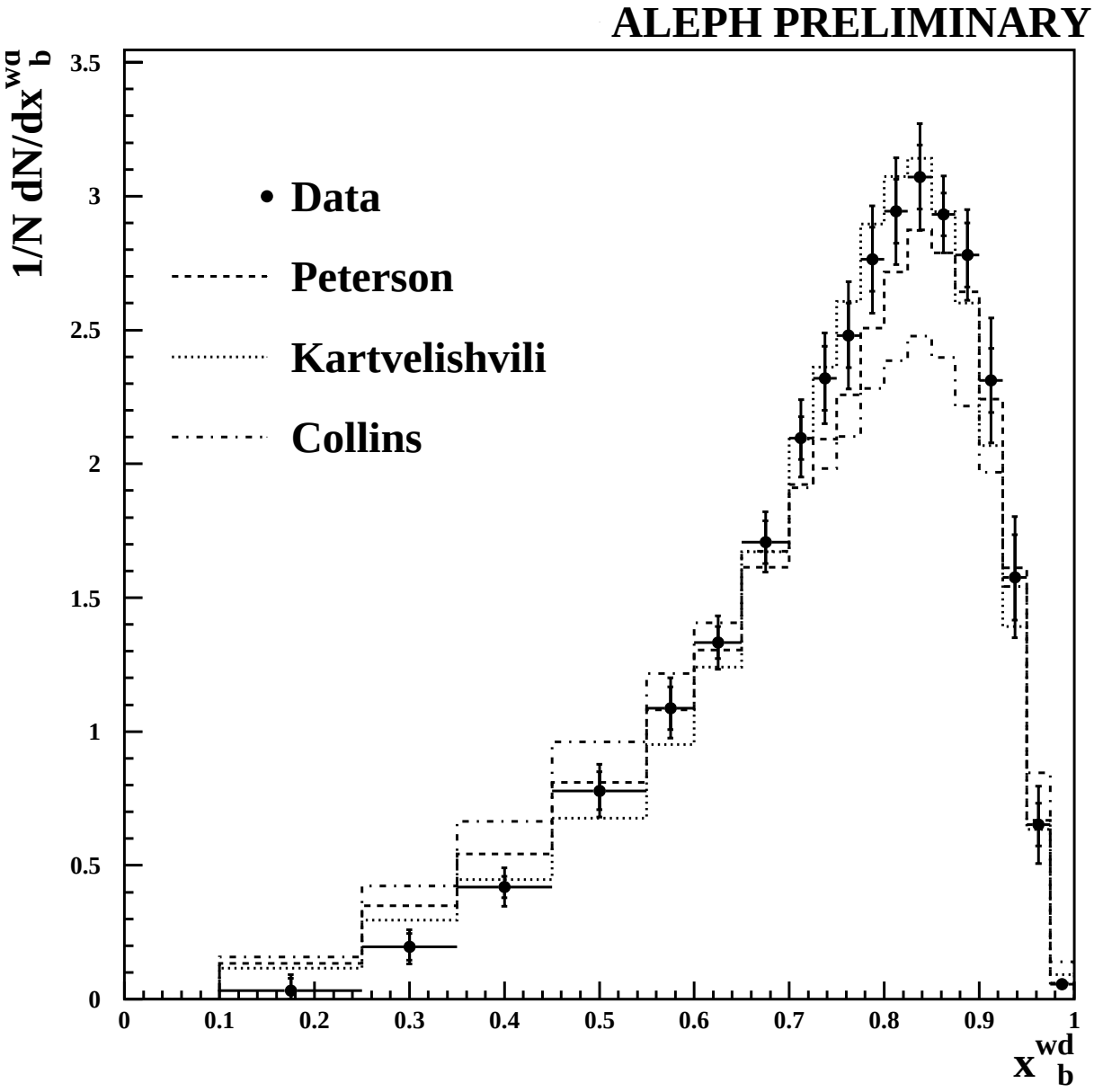

Figure 4: Reduced energy of the weakly–decaying B hadron, as reconstructed from data. The smaller error bars are statistical, the wider total errors. The best–fit distributions for Peterson[5], Kartvelishvili[6] and Collins[7] are superimposed.

Table 7: The $f_i\left(x_b^{\rm wd}\right)$ binned distribution.

Bin	Range	$f_i\left(x_b^{\rm wd}\right)$
1	$0-0.1$	0.
2	$0.10-0.25$	$0.005 \pm 0.007 \pm 0.006$
3	$0.25-0.35$	$0.020 \pm 0.005 \pm 0.004$
4	$0.35-0.45$	$0.042 \pm 0.004 \pm 0.006$
5	$0.45-0.55$	$0.078 \pm 0.007 \pm 0.007$
6	$0.55-0.60$	$0.054 \pm 0.004 \pm 0.004$
7	$0.60-0.65$	$0.067 \pm 0.003 \pm 0.004$
8	$0.65-0.70$	$0.085 \pm 0.004 \pm 0.004$
9	$0.70-0.725$	$0.052 \pm 0.002 \pm 0.003$
10	$0.725-0.75$	$0.058 \pm 0.003 \pm 0.003$
11	$0.75-0.775$	$0.062 \pm 0.003 \pm 0.004$
12	$0.775-0.80$	$0.069 \pm 0.003 \pm 0.004$
13	$0.80-0.825$	$0.074 \pm 0.003 \pm 0.004$
14	$0.825-0.85$	$0.077 \pm 0.003 \pm 0.004$
15	$0.85-0.875$	$0.073 \pm 0.003 \pm 0.003$
16	$0.875-0.90$	$0.070 \pm 0.003 \pm 0.003$
17	$0.90-0.925$	$0.058 \pm 0.003 \pm 0.004$
18	$0.925-0.95$	$0.039 \pm 0.004 \pm 0.004$
19	$0.95-0.975$	$0.016 \pm 0.002 \pm 0.003$
20	$0.975-1.00$	$0.001 \pm 0.000 \pm 0.000$

7 Systematic checks

A number of systematic checks were performed to evaluate the stability of the measurement.

- Separate measurements with electrons or muons: the measurement of $\langle x_b^{\mathrm{L}} \rangle$ was repeated using only muons and only electrons. The results were

$$\begin{aligned} \langle x_b^{\mathrm{L}} \rangle_{\mathrm{electrons}} &= 0.755 \pm 0.009(\mathrm{stat}) \\ \langle x_b^{\mathrm{L}} \rangle_{\mathrm{muons}} &= 0.744 \pm 0.010(\mathrm{stat}) \end{aligned}$$

- Separate measurements channel by channel: the measurement of $\langle x_b^{\mathrm{L}} \rangle$ was repeated using only one channel at a time. The results are shown in Table 8.

Table 8: Separate measurements channel by channel. The errors are only statistical and uncorrelated.

Channel	$\langle x_b^{\mathrm{L}} \rangle$
1	0.738 ± 0.015
2	0.748 ± 0.015
3	0.748 ± 0.014
4	0.744 ± 0.025
5	0.762 ± 0.015

- Measurement using a $q\bar{q}$ Monte Carlo simulation instead of data: the measurement gives

$$\begin{aligned} \langle x_b^{\mathrm{L}} \rangle_{\mathrm{MC}} &= 0.713 \pm 0.005(\mathrm{stat}) \\ \langle x_b^{\mathrm{wd}} \rangle_{\mathrm{MC}} &= 0.692 \pm 0.005(\mathrm{stat}) \end{aligned}$$

  while the true values are

$$\begin{aligned} \langle x_b^{\mathrm{L}} \rangle_{\mathrm{MCtruth}} &= 0.711 \\ \langle x_b^{\mathrm{wd}} \rangle_{\mathrm{MCtruth}} &= 0.692 \end{aligned}$$

8 Conclusions

Using all LEP I statistics collected by the ALEPH experiment at the Z resonance, about 3000 semileptonic B^0 and $B^{\pm}$ decays were selected; the effective b fragmentation function has been measured. The mean value, $\langle x_b^{\mathrm{L}} \rangle$, amounts to

$$\langle x_b^{\mathrm{L}} \rangle = 0.7499 \pm 0.0065(\mathrm{stat}) \pm 0.0069(\mathrm{syst}).$$

The binned spectrum $f_i\left(x_b^{\mathrm{L}}\right)$ is also provided, and compared with the prediction of JETSET 7.4[2] with different fragmentation models. While Kartvelishvili[6] fragmentation function gives a

rather good description of the data and Peterson[5] gives an acceptable fit, Collins[7] model is not able to reproduce the data.

A similar analysis has been performed to obtain the energy distribution of the weakly decaying B hadron, $x_b^{\rm wd}$; the result for the mean value is

$$\langle x_b^{\rm wd} \rangle = 0.7304 \pm 0.0062(\text{stat}) \pm 0.0058(\text{syst}) \quad .$$

References

[1] The ALEPH Collaboration, "ALEPH: a detector for electron–positron annihilations at LEP", Nucl. Instr. Meth. **A294** (1990) 121.

[2] S. Sjöstrand, Comp. Phys. Comm. **82** (1994) 74.

[3] The ALEPH Collaboration, "Heavy quark tagging with leptons in the ALEPH detector", Nucl. Instr. Meth. **A346** (1994) 461.

[4] The ALEPH Collaboration, "Measurement of the B_s^0 lifetime", Phys. Lett. **B322** (1994) 275.

[5] C. Peterson et al., Phys. Rev. **D27** (1983) 105.

[6] V. G. Kartvelishvili et al., Phys. Lett. **B78** (1978) 615.

[7] P. Collins et al., J. Phys. **G11** (1985) 1289.

[8] ALEPH 2000-20 CONF 2000-17, contribution to *Winter 2000 Conferences*.

[9] G. Bauer et al., hep-ex/9909014.

[10] The ALEPH Collaboration, "Resonant structure and flavour tagging in the $B^{\pm}$ system using fully reconstructed B decays", Phys. Lett. **B425** (1998) 215.

[11] N. Isgur and M.B. Wise, Phys. Lett. **B232** (1989) 13.

[12] C. Caso et al, Eur. Phys. J. **C3** (1998) 1, and 1999 Web Update.

[13] LEPHFS note 99-02, in preparation.